The Development of MSn in Digitally-Operated Linear Ion Guides.

5 AUTHORS, INCLUDING:

Gregory Brabeck
Washington State University
5 PUBLICATIONS   26 CITATIONS

SEE PROFILE

Liang Wang
Washington State University
11 PUBLICATIONS   32 CITATIONS

SEE PROFILE

Peter T A Reilly
Washington State University
62 PUBLICATIONS   1,115 CITATIONS

SEE PROFILE

Development of MS^n in Digitally Operated Linear Ion Guides

Gregory F. Brabeck, Huijuan Chen, Nathan M. Hoffman, Liang Wang, and Peter T. A. Reilly*

Department of Chemistry, Washington State University, Fulmer 305, Pullman, Washington 99164, United States

ABSTRACT: This publication demonstrates the use of digital waveform manipulation in linear ion guides to trap isolated ions and fragment them before mass analysis by time-of-flight mass spectrometry (TOF-MS). Ion trapping and collection was performed by waveform duty cycle manipulation to create a negative axial potential between the rods and the end-cap electrodes. Ion isolation can be performed by duty cycle manipulation to narrow the range of stable masses while continuing to axially trap the ions. Further ion isolation can then be performed by jumping the quadrupole frequency to each side of the stability zone to eliminate ions above and below the isolated ion mass. Collision-induced dissociation was demonstrated by duty cycle manipulation to either axially or radially excite the ions. The methods for performing these types of excitations are discussed and demonstrated. These techniques can be combined or used separately for MS^n analysis. The use of frequency and duty cycle manipulation of the applied waveforms simplifies the hardware while greatly increasing the capabilities of linear ion guides and quadrupole time-of-flight mass spectrometers (Q-TOF-MS). Linear quadrupoles can now be used as high efficiency ion traps for collection, isolation, and tandem mass spectrometry at any value of m/z when operated digitally.
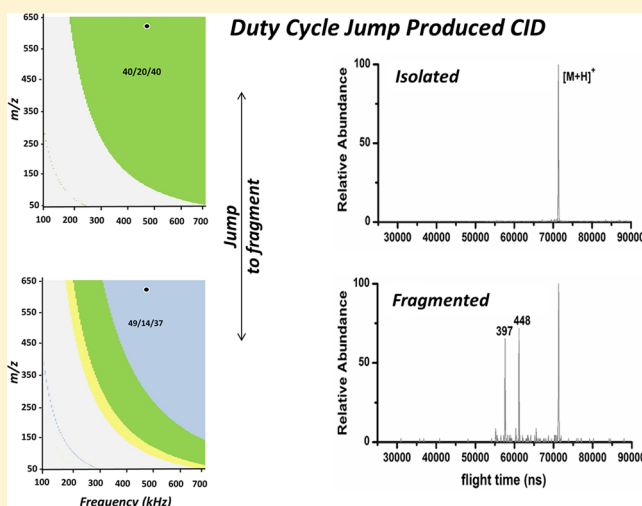
Since becoming commercially available in the mid 1990s, quadrupole time-of-flight mass spectrometers (Q-TOF-MS) have advanced through automation of instrument control and data processing and continued improvements in mass resolution, accuracy, and sensitivity. These improvements permit Q-TOF-MS to be applied to biological samples using atmospheric sampling and ionization techniques such as nanospray, microspray, and atmospheric pressure chemical ionization (APCI). Their rapid speed of analysis permits them to be used as detectors for liquid chromatography at high flow rates. Another key feature is their ability to perform tandem mass spectrometry (MS/MS) with combined high sensitivity and high mass accuracy for both precursor and product ions.

One of the drawbacks of the Q-TOF-MS is the ion sampling process. Ions from a continuous atmospheric pressure source are formed into a continuous beam with only a small portion being sampled into the flight tube for mass analysis during a "scan". In theory, the percentage of the ion beam sampled into the flight can be maximized by increasing the sampling frequency and optimizing the delay and duration of the pusher pulse. It is claimed that the ion sampling duty cycle can range between 5 and 30% depending on the m/z range of ions and the instrumental parameters.[1] In practice, users do not generally optimize the sampling duty cycle for each new sample and range. As a result, the fraction of analyte detected to the analyte injected into the TOF is usually significantly smaller than projected by the optimized instrument duty cycle. This presents a significant sensitivity loss.

Another consequence of the ion sampling process is the inability to collect and concentrate analyte ions. The solution concentration has to be within a specific range in order to produce an optimal response from the detector. This represents a challenge in protein analysis that stems from sample complexity. For example, protein concentrations in human blood plasma can vary by as much as 10 orders of magnitude.[2] The dynamic range of commercial Q-TOF-MS systems is claimed to be approximately 5 orders of magnitude under the best conditions. Consequently, there is a need to improve the analyzable concentration range.

The ion trap mass spectrometer (ITMS), on the other hand, has the ability to collect, isolate, and concentrate ions. It is the ability to control the number and range of ions being analyzed and the ability to perform MS^n that make ion traps good instruments for quantitative analysis. Automatic gain control makes ion traps useful for quantitation by adjusting the number of ions in the trap to maintain a linear detector response and negate space charge effects. They are also fast and sensitive enough to be used as detectors for chromatography. The
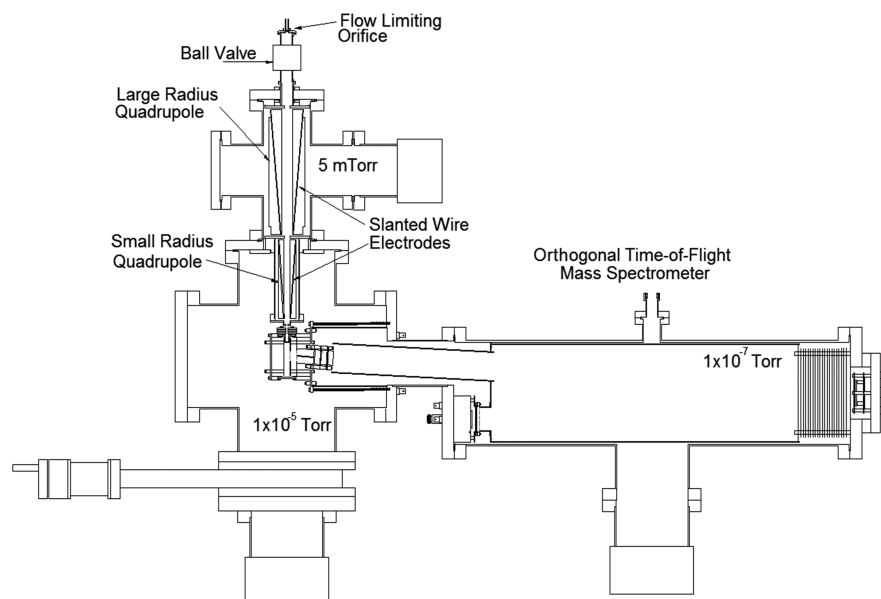
Figure 1. Instrument schematic.

resolving power of ion traps depends mostly on scan speed, with higher resolving power achieved at slower scan speeds.

Ideally, if the traits of the TOF-MS and ITMS could be appropriately mixed, then a much more powerful instrument could be obtained. The development of digital ion guides and traps has made this possible. Using ion trajectory simulations, our group showed that the digital waveforms used to drive linear quadrupole ion guides could be manipulated to produce axial trapping and ejection potentials.[3] We then demonstrated their use for producing resolved digitally operated Q-TOF-MS over the entire range of intact singly charged proteins[4] and higher.[5] Naturally, this method of axial trapping and ejection of ions works just as well at low mass as it does at high mass. We later showed through simulation that the waveforms could also be manipulated to isolate specific ions while they were axially trapped.[6] We then worked to produce spreadsheet-based programs for creating the stability diagrams needed to guide duty cycle produced ion isolation.[7] These provide a theoretical framework for experimental results from other groups mapping the stability diagram of the DIT at varying duty cycles[8] and creating a duty-cycle-based mass filter.[9]

In this publication, we present three methods for performing tandem mass spectrometry in digitally driven linear quadrupoles. The first induces collisional dissociation by energetically controlling the axial ejection and/or the injection into a gas-filled digitally operated quadrupole followed by TOF-MS analysis. The second method switches the trapping frequency or the duty cycle to move the ions out of stability region for a fixed number of cycles to increase the translational kinetic energy of the ion and then switches it back to keep the ions trapped while the translational kinetic energy is converted to internal energy by collisions. This switching process is performed repeatedly until the desired amount of fragmentation occurs. The third method moves the ion to the boundary just inside the stability region. Ions near the boundary are kinetically excited, and collisions with the buffer gas induce dissociation. The fragmented ions quickly cool because they are no longer near the boundary and remain trapped. This dissociation method permits CID to completion without significant ion loss. Fragment ions generated by any of the

three processes may be isolated and excited to perform MS^n. The ability to collect, isolate, and excite ions for subsequent mass analysis by TOF-MS vastly improves the capabilities of Q-TOF mass analyzers.

EXPERIMENTAL SECTION

The instrument schematic is depicted in Figure 1. The ions are generated at atmospheric pressure by electrospray ionization and sampled into the instrument through a flow limiting orifice. The ions and carrier gas expand into a plenum chamber that exits only into the large radius quadrupole (25.4 mm diameter rods) chamber. There is no differential pumping of the plenum chamber. Every gas molecule that enters through the flow-limiting orifice expands into the quadrupole through a 4 mm orifice whereupon the ions are caught by the quadrupole field, and the carrier gas molecules are pumped away by a 250 L/s turbo pump. The pressure in the plenum chamber is on the order of 500 mTorr. The pressure in the large radius quadrupole (LRQ) chamber is 5 mTorr.

Collisions with the buffer gas in the LRQ chamber quickly eliminate the translational kinetic energy imparted by the low pressure expansion from the plenum chamber, and the ions are stopped inside the LRQ. Slanted wire electrodes inserted between the quadrupole rods create z-axis fields that continually force the ions toward the orthogonal acceleration time-of-flight mass spectrometer (oa-TOF-MS). The waveforms of the LRQ and small radius quadrupole (SRQ) with 12.7 mm diameter rods are digitally produced and manipulated so that ions can be axially trapped or ejected on demand by either quadrupole. Digital waveform manipulation permits ion isolation and tandem mass spectrometry to be performed inside the quadrupoles followed by controlled ion injection into the oa-TOF for resolved mass analysis. This publication reveals procedures for accomplishing these tasks.

DIGITAL WAVEFORM MANIPULATION

Electrosprayed reserpine was the target molecule of this demonstration. It has a mass at m/z 609.69 (MH$^+$). The range of stability diagrams presented was selected by the

generation of MS/MS from this mass. Shifting the trapping range to essentially any value is a minor procedure. The LRQ was operated at ±200 V and a duty cycle of 47/6/47 (($t_1$100/T)/($t_2$100/T)/($t_3$100/T)). The m/z versus frequency stability diagram for this waveform is presented in Figure 2. This
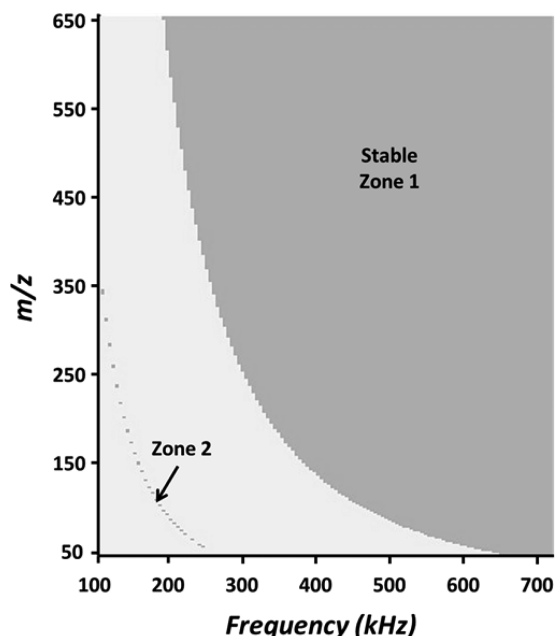

Figure 2. Stability diagram of m/z vs F for a 47/6/47 duty cycle waveform. The dark gray shaded regions are stable. The white regions are unstable.

waveform provides a symmetric quadrupole field ($t_1 = t_3$) with an axial well depth of 12 V ($D_{axial} = V^-·t_2/T$) when the end-cap electrodes are at ground potential. If the inlet is left at ground potential, this waveform can be used to trap the reserpine ions with minimal fragmentation. Fragmentation can be induced by increasing the value of $t_2·100/T$. This changes the collision energy of the ions entering the gas-filled (5 mTorr) LRQ by $E_{col} = zeV^-·t_2/T$, assuming the inlet is at ground potential. The value ze defines the ion charge. The m/z versus F stability diagram was calculated from matrix methods.[6,10−12] The program used to create this stability diagram is available for download from our group Web site: http://reilly.chem.wsu.edu/digital-waveform-stability-diagrams-2/.

Ion isolation while maintaining axial trapping may be accomplished in the LRQ by changing the duty cycle. The stability diagram for a 52/10/38 waveform is shown in Figure 3. Note that the dark gray stability region has narrowed because $t_1 \neq t_3$ while maintaining the ability to axially trap or eject ions because $t_2 \neq 0$. This diagram shows that the range of stable frequencies for the m/z 609.69 ions is approximately 202.5 to 265.0 kHz. Standard function generators have 1 Hz frequency resolution or better. The frequency can be jumped to the extremes of the stability range to eliminate the ions above and below the m/z of interest to perform precise ion isolation.

The isolated ions can now be fragmented by ejecting them into the second gas-filled digitally operated small radius quadrupole (SRQ). The collision energy is controlled by using the duty cycle of the LRQ to control the energy of ejection ($KE_{eject} = zeV^+_{LRQ}·(t_2/T)$) or by using the duty cycle of the SRQ to control the axial well depth ($D_{SRQ} = zV^-_{SRQ}·(t_2/T)$) or a combination of the two $KE_{collison} = zeV^+_{LRQ}(t_2/T)_{LRQ} +$
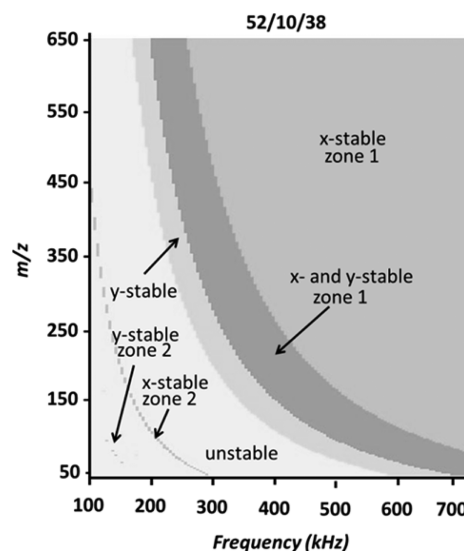

Figure 3. Stability diagram of m/z vs F for a 52/10/38 duty cycle waveform. The dark gray shaded regions are stable. The lighter gray tones are only stable along one axis. The white regions are unstable.

$zeV^-_{SRQ}(t_2/T)_{SRQ}$. If one were to limit the values of t_2/T to 0.5 for each quadrupole operating at ±200 V, the ion beam energy would be a maximum of 200 eV/z. The ability to control the collision energy with up to z·200 eV is more than sufficient for collision-induced dissociation (CID). The exit end-cap of the SRQ can be biased if needed to enhance axial trapping well depth. However, leaving it at ground potential is usually sufficient. The fragmented ions settle at a point just before the exit end-cap where the axial forces from the biased slanted wire electrodes and the duty-cycle-induced axial trapping potential balance to await axial ejection into the oa-TOF-MS.

An alternative method for performing CID can also be done inside a single linear quadrupole following the trapping and isolation procedure described above. Figure 4 reveals the stability diagram created when the duty cycle is adjusted to 48/10/42. The difference between t_1 and t_3 has been reduced to broaden the range of fragment ions (see Figure 4). Keeping the
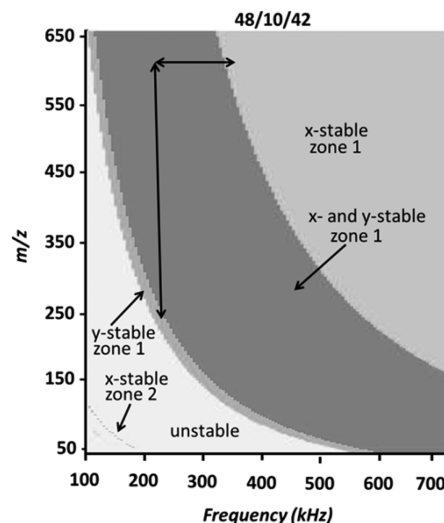

Figure 4. Stability diagram of m/z vs F for a 48/10/42 duty cycle waveform. The dark gray shaded region is stable. The lighter gray regions are stable on one of the axes. The white regions are unstable.

t_2 at 10% will maintain a sufficient axial well depth ($D_{axial} = V^- \cdot t_2/T$) of 20 V. Under these conditions, the MH$^+$ reserpine ions are stable in the SRQ from approximately 195.2 to 410.8 kHz.

In order to collisionally induce dissociation, the translational kinetic energy of the ion has to be increased. When an ion crosses into an unstable region, it quickly absorbs energy from the applied quadrupole field to eject when its kinetic energy exceeds the trapping well depth. Fortunately, that process takes multiple cycles of the trapping waveform, and the waveform generator is agile enough to apply a controlled number of cycles before switching the frequency back to a stable frequency (see the double headed horizontal arrow in Figure 4). Collisions with the buffer gas convert the ions' kinetic energy to internal energy to induce fragmentation. Note that the starting frequency is not near the edge of the stability zone so that the ions are not significantly excited by proximity to the boundary. The range of fragmented ions collected is defined by the projection of the vertical double headed arrow on to the y-axis. This CID process can be repeated until the desired level of dissociation is reached. The isolation and excitation processes may be performed on any product ion species to provide MS^n in a single linear ion guide.

Alternatively, the frequency can remain constant during the process, and excitation can be induced by changing the duty cycle. For example, ions could be trapped with the duty cycle whose stability diagram is depicted in Figure 2. Then the shape of the stability region is changed (e.g., Figure 4) by switching the duty cycle so that the target ions are no longer stable at the fixed frequency. That unstable waveform is then applied for n cycles to translationally excite the ions after which the duty cycle is switched back to the stable waveform (Figure 2), whereas the translational energy of the ions is converted to internal energy through buffer gas collisions to induce dissociation. Duty cycle switching and frequency hopping can be used to destabilize the ions and yield the same type of quadrupole field-induced excitation.

Perhaps a more subtle approach is to use the high mass boundary of the stability region[13] to induce excitation. The duty cycle is switched to introduce a high mass cutoff and a wide range of stable m/z, as depicted in Figure 4. The frequency is then shifted to place the ions just inside the stable region. As the changing frequency moves the ions toward the stability boundary, the amplitude of their stable, periodic secular oscillation increases. Once the boundary is reached, the ion oscillations become periodic but unstable. Ions just inside the boundary have the maximum allowable translational kinetic energy without detrapping. The oscillating quadrupolar field maintains this high level of translational kinetic energy while the ions undergo buffer gas collisions that increase their internal energy until they dissociate. The fragment ions are quickly cooled by collisions because they are farther from the boundary. In this way, the excitation can be applied for long periods of time (hundreds of milliseconds) without loss of the precursor ions, because they are never unstable.

■ RESULTS

To demonstrate the proof of principle of these ion manipulation processes, we have introduced electrosprayed reserpine ions into the inlet where they are passed through the LRQ and then into the SRQ to be trapped and collected for on-demand injection into the pusher of the oa-TOF-MS. The potentials of the DC power supplies that are switched by the high voltage pulsers (DEI, Inc., PVX-4150, Colorado) to create

the LRQ waveforms were + and −250 V. The duty cycle of the LRQ was set to 45/10/45. Because the inlet is grounded, the change in axis potential is −25 V. The LRQ entrance end-cap electrode was set to −10 V. The potentials of the DC power supplies that are switched by the pulsers to create the SRQ waveforms were + and −150 V. The potential of the end-cap electrode between the LRQ and SRQ was set to −27 V. The duty cycle of the SRQ was initially set to 40/20/40 yielding a DC axis potential of −30 V. Under these conditions, the ions pass directly through the LRQ and into the SRQ to be trapped and collected near the grounded exit cap electrode. The trapped ions were ejected from the SRQ into the oa-TOF for on demand mass analysis with a 45/10/45 ejection duty cycle that created a DC axis voltage of +15 V. That yielded a 15 V potential drop into the oa-TOF. Figure 5a reveals the mass
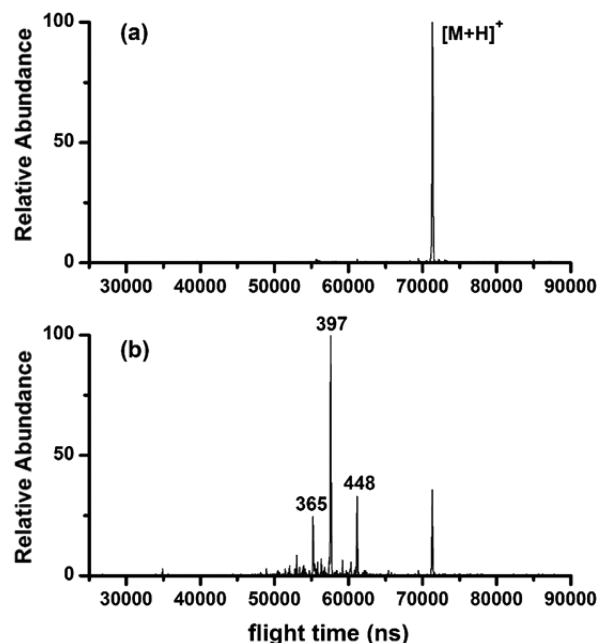

Figure 5. Tandem mass spectrometry of reserpine by duty-cycle-induced axial potential modulation. (a) Spectrum of reserpine ion after isolation in the SRQ. (b) Product ion spectrum of reserpine by varying trapping duty cycle of the SRQ.

spectrum of singly charged reserpine after it has been transferred to the SQR initially operating with a trapping 40/20/40 duty cycle. The combination of the duty cycle and the high voltage potentials of the applied rectangular waveforms yield a net −30 V potential drop between the inlet and the SRQ. As evidenced in Figure 5a, the applied potential changes were not enough to yield significant fragmentation. The t_2 value of SRQ trapping duty cycle was then increased while keeping $t_1 = t_3$ to increase the potential drop between the inlet and the SRQ. A −36 V duty-cycle-induced potential drop (38/24/38) between the inlet and the SRQ, and the same ion collection and ejection procedure used in Figure 5a was used to produce the MS/MS spectrum in Figure 5b. The ion transfer through the LRQ and into the SRQ is prompt because the LRQ was not set up to trap the ions. Therefore, the net potential drop between the inlet and the SRQ defines the collision energy. Using the duty cycle to decrease the DC axis potential of the SRQ by only 6 V was enough to produce the observed fragmentation. The duty-cycle-induced axial fragmentation procedure revealed here can be as easily performed between the inlet and a single

quadrupole, or it can be performed with each transfer into a quadrupole if the quadrupoles are used to trap the ions. This is the type of MS/MS procedure that one may use with the rapid throughput of a Q-TOF with the big advantage that the sampling duty cycle into the mass analyzer would always be near unity.

Quadrupole waveform-induced radial excitation is revealed in Figure 6. The reserpine ions were again isolated in the SRQ and
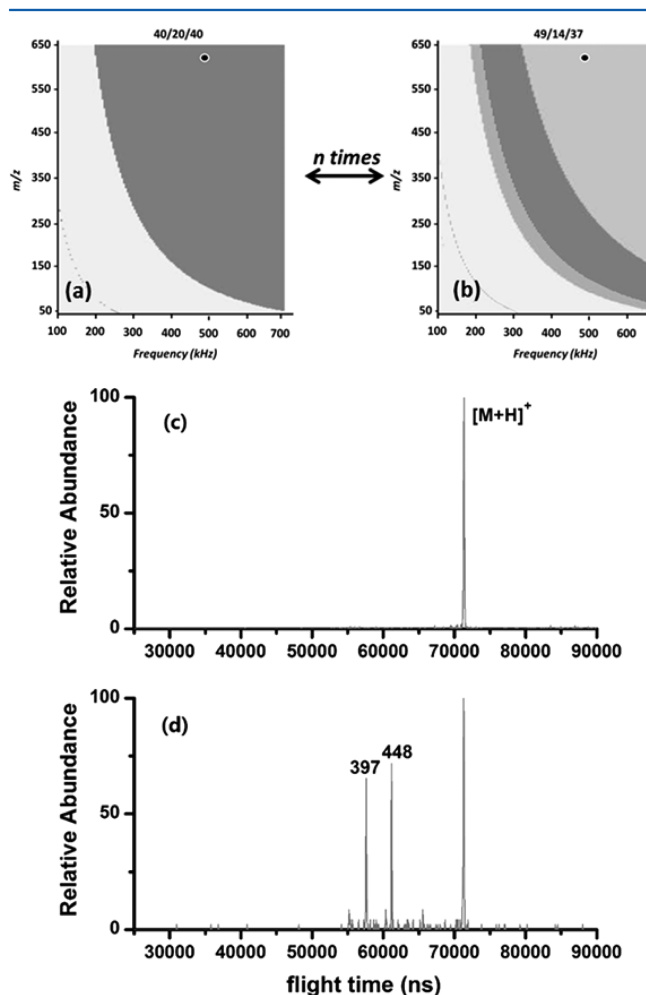

Figure 6. (a) Stability diagram of the 40/20/40 duty-cycle trapping. (b) The 49/14/37 duty-cycle stability diagram used for radial excitation of reserpine ion at 500 kHz. (c) The mass spectrum of reserpine ions without duty-cycle-induced radial excitation. (d) The CID spectrum of reserpine induced by switching the duty cycle to radially destabilize the reserpine ions for ~10 μs (five cycles at 500 kHz) and then switching the duty cycle back to restabilize the ions and allow them to undergo CID for 100 μs. This process was repeated 10 time to produce the MS/MS spectrum in (d).

collected at the end of the quadrupole using the same method previously illustrated. The trapping waveform was then set to 40/20/40 duty cycle at 500 kHz. Under these conditions, the reserpine ions are stable, as shown in the stability diagram (Figure 6a). The duty cycle was then switched to 49/14/37 where the ions are out of the stability region for 10 μs (five cycles) and then switched back to 40/20/40 where the ions are inside the stability boundary for 100 μs. The process of duty-cycle hopping of the waveform at fixed frequency was repeated 10 times to radially excite the reserpine ions and cause CID. The mass spectrum of reserpine after 40/20/40 duty-cycle

trapping but without duty-cycle-induced radial instability is shown in Figure 6c. The duty-cycle-hopping-induced MS/MS spectrum of reserpine is shown in Figure 6d.

Alternatively, after the trapping and isolation is complete, the frequency could have been jumped to approximately 300 kHz and then the duty cycle shifted to 49/14/47 (Figure 6b). Then the frequency could be jumped to 500 kHz for five cycles to excite the ions and jumped back to 300 kHz for 50 cycles to undergo CID. This process would yield an MS/MS spectrum identical to the one shown in Figure 6d because the excitation processes are equivalent.

Boundary-induced CID is also easily accomplished by a procedure that is similar to duty-cycle-induced destabilization. The setup is the same as that for Figure 6. The difference is the method of radial excitation. Once again, the frequency is held constant at 500 kHz, and the duty cycle is changed to 47/10/43 to move the stability boundary near the reserpine ions without moving them into the unstable region (see Figure 7b). In this
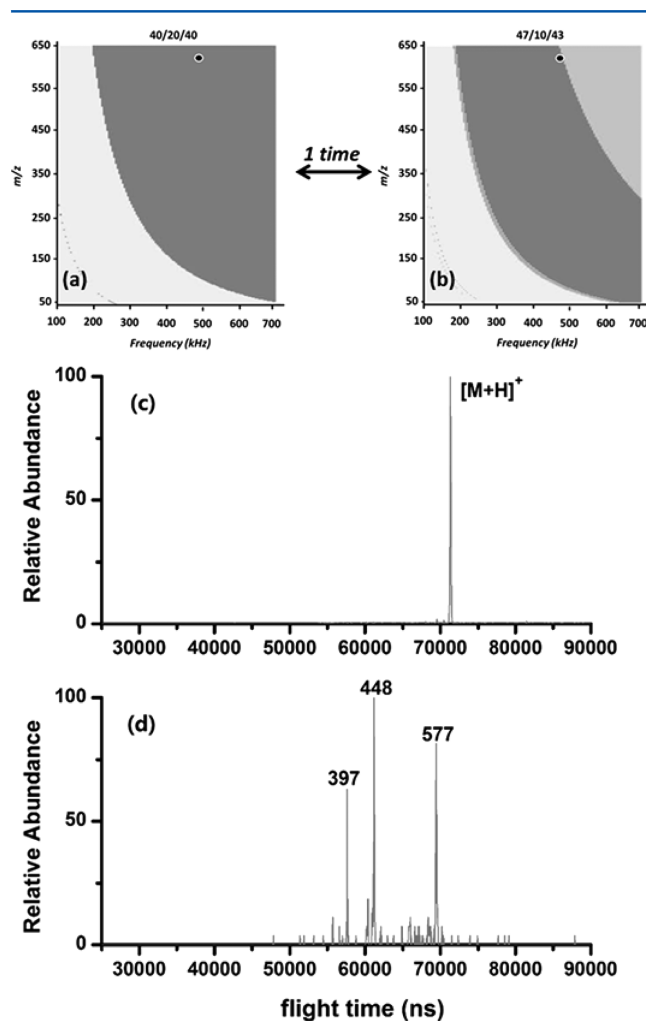

Figure 7. (a) Stability diagram for the 40/20/40 duty-cycle trapping. (b) The 47/10/43 duty-cycle stability diagram used for radial excitation of reserpine ion at 500 kHz at the boundary. (c) The mass spectrum of reserpine ions without duty-cycle-induced radial excitation. (d) The CID spectrum of reserpine induced by switching the duty cycle to radially destabilize the reserpine ions for ~100 ms at 500 kHz and then switching the duty cycle back to restabilize the ions and allow them to cool for X μs before injecting them into the TOF to produce the MS/MS spectrum in (d).

case, the reserpine ions remain stable, but because they are near the boundary they are radially excited, though not enough to detrap. Because they cannot be ejected by this procedure, the excitation can be sustained for long periods. Any fragments are stabilized away from the boundary. This procedure was applied for 100 ms to completely fragment the reserpine ions as shown in Figure 7d. Interestingly, this procedure appears to be gentler than the procedures that destabilize the ion for short periods because of the presence of the m/z 577 ions that are not present in any of the other methods of excitation.

■ DISCUSSION

The above results show that digitally driven linear ion guides can be operated as ion traps and perform MS/MS by controlling the change in the DC axis potential in moving the ion into a gas-filled quadrupole (collision cell) in a similar manner to that used by standard Q-TOFs. The difference in this case is that waveform duty cycle instead of a separate power supply is used to create the DC axis potential change to energize the ions as they pass into a collision cell. Duty-cycle-based manipulation of the DC axis potential simplifies the hardware (fewer power supplies) while adding agility because the waveform response is essentially instantaneous.

We have also demonstrated that MS/MS can be performed in a single quadrupole by digital manipulation of the trapping waveforms. Our stability diagram calculations show that manipulation of the duty cycle can be used to create a high mass boundary and narrow the range of stable masses. We have shown that translating the ions from the stable zone into the unstable region for short periods (a few trapping waveform cycles) and then back can be used to induce CID. Translation of the ions into the unstable region can be obtained by hopping the trapping frequency to move the ions into the unstable region or it can be accomplished by using the duty cycle to move the boundary so that the ion is no longer stable at the applied frequency. Both methods are essentially equivalent. The short sojourn into the region of instability allows the ions to rapidly absorb energy from the applied quadrupolar field. The duration of the jump into the unstable region is limited to a fixed number of cycles so that the ions will translationally excite without leaving the vicinity of the central axis of the quadrupole. The frequency/duty cycle is then jumped back into the stable region for n cycles to allow the field-induced translational energy to be converted to internal energy through collisions with the buffer gas. The advantage of this technique is that it permits broadband excitation, and the ions do not need to be collected at a single point so the large ion capacity of the linear trap can be fully utilized. On the other hand, boundary-induced CID is best performed when the ions are collected at a single point along the quadrupole axis, and it is useful for exciting only a narrow range of masses. The advantage of this method of inducing CID is that it is easy to push it to completion without worrying about the duration of the excitation inducing ion loss.

Perhaps the greatest advantage of digitally over sinusoidally driven devices is that there is no mass range limitation. We have shown that millions of singly charged ions up to m/z 3×10^9 Da can be trapped in our digitally operated linear ion guides.[14] We claim that when statistically significant numbers of ions can be trapped, they can be mass analyzed with high resolution and/or collisionally excited by digital waveform manipulation. Naturally, whether or not they undergo dissociation depends on the nature of the ions and not the collision-induced

excitation process. The mass limitation of sinusoidal devices results from the use of resonantly tuned circuits to create the waveform and select ions by varying the amplitude. Resonantly tuned circuits require fixed frequencies. The ability to precisely vary the trapping frequency allows the trapping range to be moved to any desired value. Consequently, digital production of the waveforms extends the mass range of the Q-TOF. Moreover, we have shown that duty cycle manipulation of digitally produced waveforms is part of the critical technology that enables ultrahigh mass ions ($m/z > 20,000$) to be trapped, manipulated and mass analyzed with high resolution.[3−5,14,15]

The work presented here shows the promise of digitally driven linear ion traps to yield an instrument with all the advantages of linear ion guides and 3D ion traps without their respective disadvantages. For example, unlike in 3D ion traps, the ions in a digital linear quad do not have to traverse an RF barrier to enter the quadrupolar region; therefore, the trapping efficiency is much higher. Unlike the sinusoidally driven quadrupoles used in commercial Q-TOFs, digitally driven quadrupoles can trap and collect ions to preconcentrate them before mass analysis; therefore, the sampling duty cycle can be set near unity.

Additionally, quadrupole mass filter resolution is geometrically limited by the variation in the radius r_0 along the length of the device. Variations in r_0 along the entire length of the device result in variations in the range of stable masses. Ions must traverse the length of the quadrupole to be detected. This does not have to happen in a linear quadrupole ion guide when it is used as a digitally operated ion trap. In this case, the ions can be collected in a compact cloud before the end-cap electrode where mass isolation and CID can occur.[3] The value of r_0 does not change appreciably over the tiny length of the ion packet. Therefore, digital operation of a linear guide as an ion trap does not have the same geometric limitations on mass resolution that occur when they are operated as mass filters. Moreover, mass isolation by digital waveform manipulation yields much better resolution than operating the quadrupole as a mass filter because the trapping frequency control is much more precise (up to 48 bit precision with direct digital synthesis) than adjusting the ratio of the AC and DC voltages.

■ CONCLUSION

Our work convincingly shows that using digitally driven quadrupoles vastly improves the capabilities of Q-TOFs. Because digital waveform manipulation allows the ions to be continuously trapped and concentrated before mass analysis is performed, the sampling duty cycle is no longer an issue for Q-TOFs. That is to say that the linear quadrupoles can collect, isolate, and now perform CID with the same facility as any ion trap. Unlike sinusoidally operated Q-TOFs, their digitally operated cousins can perform MS^n. Digital operation of the Q-TOF greatly extends the mass range as well. The improvement in capabilities demonstrated by digital operation of the quadrupole suggests that digitally operated Q-TOFs will become the norm.

■ AUTHOR INFORMATION

Corresponding Author
*E-mail: pete.reilly@wsu.edu.

Notes
The authors declare no competing financial interest.

■ **REFERENCES**

(1) Chernushevich, I.; Loboda, A. V.; Thomson, B. A. *J. Mass Spectrom.* **2001**, *36*, 849−865.

(2) Hortin, G. L.; Sviridov, D. *J. Proteomics* **2010**, *73*, 629−636.

(3) Lee, J.; Marino, M. A.; Koizumi, H.; Reilly, P. T. A. *Int. J. Mass Spectrom.* **2011**, *304*, 36−40.

(4) Lee, J.; Chen, H.; Liu, T.; Berkman, C. E.; Reilly, P. T. A. *Anal. Chem.* **2011**, *83*, 9406−9412.

(5) Chen, H. J.; Lee, J.; Reilly, P. T. A. *Proteomics* **2012**, *12*, 3020−3029.

(6) Singh, R.; Jayaram, V.; Reilly, P. T. A. *Int. J. Mass Spectrom.* **2013**, *343−344*, 45−49.

(7) Brabeck, G. F.; Reilly, P. T. A. *Int. J. Mass Spectrom.* **2014**, *364*, 1−8.

(8) Bandelow, S.; Marx, G.; Schweikhard, L. *Int. J. Mass Spectrom.* **2013**, *353*, 49−53.

(9) Brancia, F. L.; McCullough, B.; Entwistle, A.; Grossmann, J. G.; Ding, L. *J. Am. Soc. Mass Spectrom.* **2010**, *21*, 1530−1533.

(10) Pipes, L. A. *J. Appl. Phys.* **1953**, *24*, 902−910.

(11) Richards, J. A.; Huey, R. M.; Hiller, J. *Int. J. Mass Spectrom. Ion Phys.* **1973**, *12*, 317−339.

(12) Konenkov, N. V.; Sudakov, M.; Douglas, D. J. *J. Am. Soc. Mass Spectrom.* **2002**, *13*, 597−613.

(13) March, R. E. *J. Mass Spectrom.* **1997**, *32*, 351−369.

(14) Wang, X.; Chen, H.; Lee, J.; Reilly, P. T. A. *Int. J. Mass Spectrom.* **2012**, *328−329*, 28−35.

(15) Lee, J.; Marino, M. A.; Koizumi, H.; Reilly, P. T. A. *Int. J. Mass Spectrom.* **2011**, *304*, 36−40.